
This manuscript has been submitted for publication in GEOPHYSICAL RESEARCH LETTERS. Please note that the manuscript has not yet formally undergone peer review. Subsequent versions of this manuscript may have slightly different content. If accepted, the final version of this manuscript will be available via the 'Peer-reviewed Publication DOI' link on the right-hand side of this webpage. Please feel free to contact any of the authors; we welcome feedback.

Changing under-ice thermodynamics

Title: Shortening ice seasons and changing phenology affect under-ice lake thermal dynamics

Running head: Changing under-ice thermodynamics

Author names: Isabella A. Oleksy^{*a}, David C. Richardson^b

Affiliations:

^a Department of Zoology and Physiology, University of Wyoming, Laramie, USA

^b Biology Department, SUNY New Paltz, New Paltz, NY, USA

*Corresponding author

Abstract:

Temperate lakes worldwide are losing ice cover but the implications for under-ice thermal dynamics are poorly constrained. Using a 90-year record of ice phenology from a temperate lake, we examined trends, variability, and drivers of ice phenology. The onset of ice formation decreased by 23 days century⁻¹ which can be largely attributed to warming air temperatures. Ice-off date has become substantially more variable with spring air temperatures and cumulative February through April snowfall explaining over 80% of the variation in timing. As a result of changing ice phenology, total ice duration contracted by a month and more than doubled in inter-annual variability. Using weekly under-ice temperature profiles for the most recent 36 years, shorter ice duration decreased winter inverse stratification and extended the spring mixing period.

Scientific Significance Statement:

Lakes worldwide are losing ice cover in response to climate change. We used a rare and nearly century-long dataset of ice formation and ice clearance records to examine trends, variability, and drivers. We found that ice cover is getting substantially shorter and more variable with winter ice duration about a month shorter now than it was a century ago. Using under-ice temperature measurements from the most recent three decades, we found differences in under-ice temperatures affected by lake ice duration.

Keywords: phenology; lake ice; variability; climate change; long-term trends; trend analysis

Data availability statement:

Data and metadata will be made available in an EDI data repository upon acceptance. Under-ice temperature profile data are published in Mohonk Preserve et al., 2020. Daily air temperature and precipitation data from the Mohonk Preserve Weather station are available from the US Weather Bureau/National Weather Service rain gauge (Network ID GHCND:USC00305426).

Introduction

Ice cover is one of the longest-measured indicators of climate change in lake ecosystems (Magnuson et al., 2000; Robertson et al., 1992). Widespread changes in lake ice phenology are occurring around the world (Sharma et al., 2019), and many seasonally ice-covered lakes are projected to transition toward either intermittent or complete loss of ice cover due to global anthropogenic climate change (Woolway, Sharma, et al., 2022). Lake ice and the timing of its formation and clearance affect many lake ecosystem properties such as oxygen dynamics, the timing of thermal stratification, and lake productivity (Adrian et al., 1999; Jansen et al., 2021; Prowse et al., 2011). Understanding under-ice thermal dynamics is crucial to further comprehending the impacts of changing ice phenology on lake ecosystems.

Two distinct phases of lake thermal dynamics under ice have been currently identified and are dependent on lake morphometry and local climatic conditions (Kirillin et al., 2012). The first phase is characterized by the release of heat from the sediments that have accumulated in the ice-free season. The second phase is typically characterized by inverse stratification, although it is important to note that some exceptions exist, such as in shallow lakes that are cold and fully mixed at ice-onset (cryomictic; Yang et al., 2021). Modeling exercises predict that under several Representative Concentration Pathways (RCPs), we can expect a substantial shortening of inverse stratification duration in ice-covered lakes (Woolway, Denfeld, et al., 2022).

Predicting how ongoing changes in lake ice phenology will alter annual, whole-lake ecosystem function first requires an understanding of the drivers of trends and variability around those trends (Wilkinson et al., 2020). While lake ice phenology records are common, observations of multi-decadal under-ice thermal properties are comparatively rare (e.g., Sharma et al., 2022). Under-ice temperatures are critical in contextualizing the physical, chemical, and biological implications of increasingly shorter and potentially variable ice phenology. To that

end, we analyzed a 90-year record of both ice-on and ice-off observations from a small lake in Shawangunk Mountains, New York, USA. We combined the long-term ice phenology record with weekly under-ice thermal profiles from the most recent 36 years to ask the following questions. First, are ice phenology and variability changing? Second, what local meteorological and global scale climatic variables explain variability in lake ice phenology? Third, how does ice phenology affect underwater winter stratification, temperature, and mixing dynamics?

We expected to find long-term trends in all aspects of ice phenology (ice-on, ice-off, and ice duration). We hypothesized that the timing of ice formation would be primarily controlled by minimum air temperatures in the late fall and early winter, while ice-off would be controlled by a combination of spring air temperatures and cumulative precipitation as snow. We tested the hypothesis that a combination of long-term global climate anomalies and large-scale atmospheric circulation patterns (teleconnections) would explain this interannual variability in ice duration (Beyene & Jain, 2015). Finally, we expected that the timing of ice-on and ice-off (and thus ice duration) would affect the under-ice heat content and reduce the strength of inverse stratification.

Methods

Site description and data collection

Mohonk Lake (41.766°N, -74.158°W, 379 m elevation above sea level) is a small (6.9 ha), deep (18.5 m maximum depth), dimictic, oligo-mesotrophic lake located on the Shawangunk Ridge, New York State, USA (Oleksy & Richardson, 2021; Richardson et al., 2018). The lake occupies a small glacier-formed depression in a watershed of 17.3 ha and a drainage ratio of 2.5 (Richardson et al., 2018). Ice-on day was recorded as the first day with 100% ice coverage; ice-off day was recorded as the first day with 0% ice cover from 1932-2022. In the 2018-2019 winter, there was a gap with ice melt between 23Dec2018 and 11Jan2019; to be consistent with

past records, we used the first observation of ice-on and the last observation of ice-off for these analyses. Ice phenology was recorded in a consistent manner over the entire 90-year data record with only seven years missing ice-on data (all before water year 1954) and one year of missing ice-off record in water year 1965. Over the entire ice record, maximum, minimum, and average daily air temperature (°C) and snow and precipitation (mm) were measured at a local National Weather Service station (Network ID: GHCND:USC00305426). From 1985-2022, profiles of lake temperature were taken weekly at 1m increments. Temperatures were linearly interpolated to daily timescales except if there were more than 14-day gaps in records.

Ice phenology trends analysis

All statistical analyses and data visualizations were conducted in R version 4.2.1 (R Core Team, 2022). For the three ice phenology metrics, we calculated Theil-Sen's slopes using formulas from both *zyp* and *trend* packages (Bronaugh & Consortium, 2019; Pohlert, 2020). To test if a trend was significant, we used the Mann-Kendall rank-based z-score and compared the p-value from that z-score to $\alpha = 0.05$.

To test whether variability of ice is increasing, we used two techniques. First, we calculated the standard deviation (sd) of all possible sequential windows from 4 up to 30 years if > 95% of the years had ice phenology data (Figures S1-S4). For each series across all sequential windows, we calculated Theil-Sen's slopes and intercepts to determine if sds were changing (Figures S1-S3). We averaged all slopes for each sequential window and then compared the averaged slopes to zero using one-sample t-tests. Second, for visualization, we calculated Bollinger Bands which are one standard deviation above and below a simple moving average and can indicate volatility of a time series (Bollinger, 1992).

Predictors of ice phenology

For predictors of ice phenology, we calculated the cumulative sum of rain or snow and air temperature data at one-, two-, and three-month intervals for October-December (ice-on) and February-April (ice-off). We further calculated fall and spring isotherm dates as the day when a moving average of air temperature crossed a temperature threshold (*sensu* Higgins et al., 2021). We calculated isotherm date for a factorial design using a range of daily air temperature metrics (minimum, mean, maximum), lengths of time (1 to 30 days), and temperature thresholds (0 to 5°C) for 540 unique combinations. We selected the isotherm variable that maximized R^2 for either ice-on or ice-off. The maximum observed air temperature 17 days after 0°C air temperature isotherm was crossed in late winter (hereafter “fall isotherm date”) was strongly correlated with ice-on, and the annual date that the daily 29-day mean observed air temperature crossed 4°C (hereafter “spring isotherm date”) was strongly correlated with ice-off.

We modeled ice-on and ice-off using generalized additive models (GAMs) comprised of terms that accounted for interannual variability across each time series using a gamma family with a logistic link function (Hastie & Tibshirani, 1987; S. N. Wood, 2017). We built candidate models based on the top 10 climatic variables that were most highly correlated with either ice-on or ice-off while minimizing collinearity (Figure S4). We fit several GAMs for each ice phenological variable (Table S1) and ultimately selected the models that had the lower AIC and maximized deviance explained (Table S2). We estimated GAMs using the *mgcv* package (version 1.8-40; Wood, 2019), visualized all results with the *ggplot2* package (Wickham, 2016), and arranged the plots with *patchwork* package (Pedersen, 2022).

To examine the effects of broader-scale meteorological factors, we built GAMs including global temperature and teleconnections as potential drivers of ice duration. We obtained global annual temperature anomalies averaged over land and ocean from the National Oceanic and Atmospheric Administration (NOAA, 2020). We also considered monthly NAO indices as a

predictor of ice phenology, which we downloaded from the National Weather Service Climate Prediction Center (National Weather Service, 2020).

Structural equation modeling for under-ice conditions

We constructed a model that linked ice variables (ice-on and ice-off dates) with fall and spring mixing period lengths and underwater parameters using structural equation modeling (Grace et al., 2010). For each annual under-ice period, we calculated the mean temperature in the shallow (1-3m) and deep water zones (10-12m). To estimate the magnitude of inverse stratification under ice, we calculated the difference in water density between 1m and 11m (Δ density). We also calculated the mean heat content by calculating daily heat content in the lake using the temperature profile (Wetzel et al., 2000) and took the average across the under-ice period for each year. We also calculated the length of the fall mixed period as the number of days between lake turnover and ice-on and the spring mixed period as the number of days between ice-off and the onset of summer stratification (Oleksy and Richardson 2021). To account for varying magnitudes of ranges, we mean-centered and unit-variance scaled all variables. We built model relationships in a temporally linear fashion from fall to winter to spring to include regressions with causal relationships and covariances between variables that we expected to be colinear rather than causal. To visualize relationships from the optimal SEM, we calculated partial residual plots by calculating the residuals for each variable using the multiple regression equation from the SEM. We also plotted the component and component plus residual to show where the fitted regression line was located (Wood, 1973). All SEM statistics were calculated using the *lavaan* package (Rosseel, 2012) and visualizations were created using the *semPlot* (Epskamp, 2022), *ggplotify* (Yu, 2021), *ggnetwork* (Briatte, 2021), and *cowplot* (Wilke, 2020) packages.

Results

Between 1932 and 2022, ice-on dates ranged between December 5th to February 8th with a median of December 27th. Ice-off dates ranged between March 11 and May 2 with a median of April 9th. We observed that ice-on is trending later (slope = 23 days century⁻¹, $p = 0.001$, Figure 1) but we did not detect a long-term trend in ice-off over the 90-year period of record (slope = -6.0 days century⁻¹, $p = 0.13$, Figure 1). Consequently, ice cover duration is getting shorter (slope = -32 days century⁻¹, $p = 0.002$, Figure 1). Across all the possible segment sizes ($n = 4$ to 30 years, Figure S4), ice-on standard deviation increased significantly by 7.0 days century⁻¹ ($p < 0.001$, minimum slope = 2.3 days century⁻¹, maximum slope = 11.7 days century⁻¹, Figure 2d). Ice-off standard deviation increased significantly by 2.8 days century⁻¹ ($p < 0.001$, minimum slope = 1.6 days century⁻¹, maximum slope = 5.0 days century⁻¹, Figure 2e). Ice duration variability increased significantly by 14.5 days century⁻¹ ($p < 0.001$, minimum slope = 11.5 days century⁻¹, maximum slope = 19.6 days century⁻¹, Figure 2f).

Late fall and early winter temperatures were strong controls on the timing of ice-on in Mohonk Lake (Figure 3). The best GAM explained 67.5% of the deviance in the ice-on date and included a positive linear relationship with the timing of the fall isotherm (Figure 3a, Table S2). A smaller proportion of the variance in ice-on day of year (DOY) could be attributed to cumulative daily mean air temperature in November (Figure 3b). The fall isotherm date has shifted 2.1 days decade⁻¹ later since the beginning of the ice monitoring record ($p = 0.02$; Table S3) but there was no trend in cumulative mean daily November air temperature ($p > 0.05$; Figure S6).

Ice-off was controlled by a combination of late winter and spring precipitation and air temperature variables. The best GAM explained 81.3% of the variation in the ice-off date (Table S2). The spring isotherm had a largely positive, linear effect on ice-off DOY (Figure 3c). Cumulative mean daily air temperature in February also had a substantial effect on ice-on DOY, with warmer years resulting in earlier ice-off (Figure 3d). The amount of snowfall between

February and April had a positive, non-linear impact on ice-off DOY, such that years with greater amounts of snow were associated with later ice-off, but above a certain snowfall threshold, ice-off DOY is unaffected (Figure 3e). The spring isotherm shifted earlier by 1.4 days decade⁻¹ ($p = 0.001$, $\tau = -3.24$), and cumulative mean daily air temperature in February increased by 5.9°C decade⁻¹ ($p = 0.02$, $\tau = 2.21$), but cumulative snowfall between February and April did not change substantially (Table S3).

Variation in ice duration was partially explained by trends in global temperature anomaly and variability in November and December NAO cycles (Figure 4, deviance explained 24%). Higher global temperature anomalies since the early 20th century were associated with shorter ice duration. Years with negative November and December NAO indices were also correlated with shorter ice duration.

The selected SEM converged (Figure 5a) with a comparative fit index indicating improvement over the null model (Table S4). Longer fall mixing was correlated with later ice-on dates (coefficient = 0.84, $p = 0.002$, Figure 5b). Later ice-on dates resulted in lower deep (coefficient = -0.43, $p = 0.012$, Figure 5c) but were not related to shallow average temperatures under ice (coefficient = -0.23, $p = 0.23$). Warmer deep temperatures resulted in more negative water density differences (coefficient = -0.87, $p = 0.016$, Figure 5d) while warmer shallow temperatures resulted in small water density differences (coefficient = 1.27, $p < 0.001$). Warmer shallow (coefficient = 0.61, $p < 0.001$) and deep (coefficient = 0.43, $p < 0.001$) temperatures resulted in higher mean heat content. Ice-off date was negatively correlated with the length of the spring mixing period (coefficient = -0.49, $p = 0.015$, Figure 5e).

Discussion

Mohonk Lake experienced decreases in winter ice-cover that amounted to a loss of approximately one month of winter ice cover over a 90-year period. Trends in ice duration in Mohonk Lake were driven largely by later ice formation and not earlier clearance; although ice-

off was not trending earlier, interannual variability in ice-cover increased as in many other seasonally ice-covered lakes (Benson et al., 2012). Overall, decreased ice duration was related to the interplay between global climate change and teleconnections which influenced local weather drivers, and in turn ice phenology. Specifically, shorter ice duration was associated with higher global temperature anomalies, which were captured in variables such as increasing fall, winter, and spring air temperatures (Table S3). Additional variation in ice duration was explained by the North Atlantic Oscillation (NAO) in November and December. In winters with positive NAO, the northeastern U.S. experiences mild winters while negative NAO is associated with cold-air outbreaks and strong storms, which may promote earlier ice formation or thicker ice cover, respectively. Teleconnections like El Niño-Southern Oscillation and NAO have been similarly shown to modify both ice phenology and summer stratification in lakes (Bai et al., 2012; Oleksy & Richardson, 2021; Sharma & Magnuson, 2014). For example, winter NAO has a substantial effect on spring hypolimnetic temperatures that ultimately carry into the stratified period in deep European lakes (Dokulil et al., 2006).

In Mohonk Lake, ice-on and ice duration changed twice as fast compared to means from other northern hemisphere lakes (Sharma et al., 2021) and the high rate of change was similar to lakes in the central Rocky Mountains and the Alps, which are experiencing some of the most rapid lake ice losses globally (Christianson et al., 2021; Kainz et al., 2017). The rapid change in ice phenology was tightly linked to regional and local climatic shifts. The date when air temperature crossed thresholds that precipitated ice formation (e.g., 0°C) was getting later each late fall and early winter. Consecutive cold days, in combination with cumulative mean daily temperature in November, explained about two-thirds of the variability in ice formation timing on Mohonk Lake, and have resulted in substantially later ice formation over time. Wind speed is another critical factor explaining lake ice formation; wind can modulate lake heat transfer (Read et al., 2012) and disrupt ice formation when it is still thin (Kirillin et al., 2012), but is missing from our model due to a lack of data availability.

While ice-off timing in the spring hasn't trended earlier as we expected, it has been growing increasingly more variable in recent decades; preceding seasonal weather patterns explained the majority of that interannual variability. Ice-off in Mohonk was controlled by a combination of late winter and early spring air temperatures and cumulative snowfall, consistent with mountain lakes (Caldwell et al., 2021; Preston et al., 2016; Smits et al., 2021). Warmer conditions in late winter and spring and increases in solar radiation can accelerate ice break-up (Sharma et al., 2013), but this relationship is likely modified by the amount of precipitation that falls on the lake, particularly as snow. In years with more snowfall, lake ice likely persists longer because it is thicker and has higher albedo with the accumulation of snow and associated cold temperatures, thus promoting thicker ice formation (Cavaliere et al., 2021; Kouraev et al., 2007).

Changing ice conditions impacted under-ice water temperatures in several ways. Since Mohonk is a bedrock-constrained lake in a small watershed with no surface or groundwater inflows, snowmelt likely plays a minimal role in regulating under-ice mixing as in mountain lakes (Smits et al., 2020) or groundwater intrusion lakes (Kirillin et al., 2012). Instead, under-ice thermal dynamics are likely regulated by a combination of ice duration and ice clarity which determine the degree of radiation-driven convection and mixing (Bruesewitz et al., 2015; Cavaliere et al., 2021). Later ice formation was associated with lower deep average water temperatures and thus resulted in cooler, well-mixed water columns that did not inversely stratify (Woolway, Denfeld, et al., 2022). In Mohonk Lake, in winters with shorter ice duration (driven by later ice-on), under-ice inverse stratification was weaker and ice-off occurred earlier. This will shorten the phase of stable inverse stratification under the ice (Kirillin et al. 2012; Bruesewitz et al. 2015). The phase before ice-off occurs in the spring can both last weeks or longer with deepening convective layers driven by clear ice and cycles of daily solar radiation (Bruesewitz et al., 2015; Kirillin et al., 2012; Yang et al., 2017).

While none of the under-ice thermal metrics were causally linked to ice-off date, our results point to the potential for ice phenology to impact spring thermal dynamics (Dugan, 2021; Oleksy & Richardson

Li et al., 2022). In years with longer ice seasons, the lake quickly stratified following ice clearance. Although mixed period in the spring was shorter, the onset of stratification was indeed later than average (Oleksy & Richardson, 2021). In contrast, when ice clearance occurred earlier, the spring mixing period was longer but the onset of stratification was earlier than average, with stronger stratification strength at the peak of summer (Oleksy & Richardson 2021).

Through changes in thermal dynamics, the loss of lake ice has the potential to alter many different biogeochemical and ecological dynamics in lakes. With later ice formation in the fall, more phytoplankton can grow and increase zooplankton overwintering success, dampening the spring phytoplankton bloom (Hébert et al., 2021). In spring, antecedent winter conditions alter the successional dynamics of phytoplankton assemblages and in turn can result in mismatched phenology of herbivorous zooplankton (Hrycik et al., 2022). With longer mixed seasons and earlier onset of stratification, Mohonk Lake would likely have exacerbated mismatches of zooplankton and phytoplankton spring phenology. Additionally, shorter duration of ice cover and thinner ice promotes higher under-ice metabolism which can account for a substantial amount of annual net ecosystem production (e.g., Brentrup et al., 2021).

While Mohonk Lake is likely not at risk of transitioning from dimictic to monomictic in the next century, the potential for winters with shortening ice phases, intermittent, or no ice cover is within the realm of possibility (Sharma et al., 2019, 2021). Winter limnological studies like this one are critical in “closing the loop” between under-ice and ice-free seasons (Salonen et al., 2009), and underscore the repercussions of changing winter ice phenology on lake ecosystem dynamics.

Figures

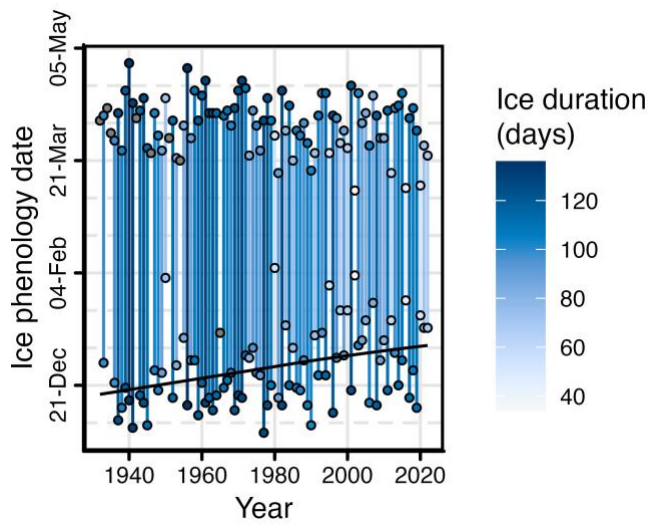


Figure 1. Ice phenology in Mohonk Lake from 1932-2022. Dates of ice-on and ice-off are plotted as points. A line segment connects the ice-on and ice-off in the same water year and the length and color gradient and point fill correspond to ice-cover duration. The black line indicates significant Theil-Sen's slope ($p < 0.05$). Filled grey points indicate years where only ice-on or ice-off was recorded.

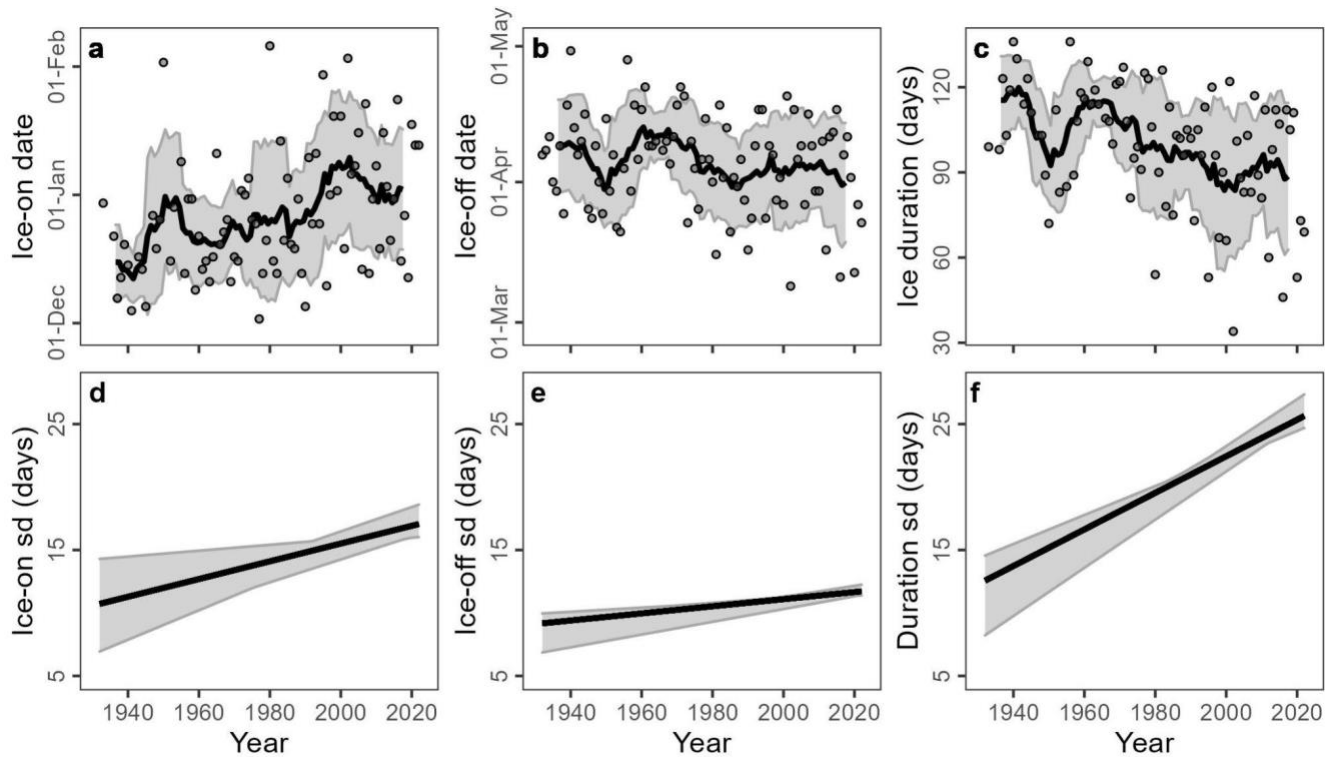


Figure 2. Ice phenology in Mohonk Lake from 1932-2022 for (a) ice-on, (b) ice-off, and (c) ice duration. For each figure, the 9-year simple moving average is presented as the dark line, and the Bollinger band (± 10 -year rolling standard deviation) is the shaded area presented at the median year for each 10-year window. Standard deviations for mean trends (slope and intercept) across all sequential windows (4 to 30 years) for (d) ice-on, (e) ice-off, and (f) ice duration with shaded areas representing minimum to 95% possible trend line fits for each year.

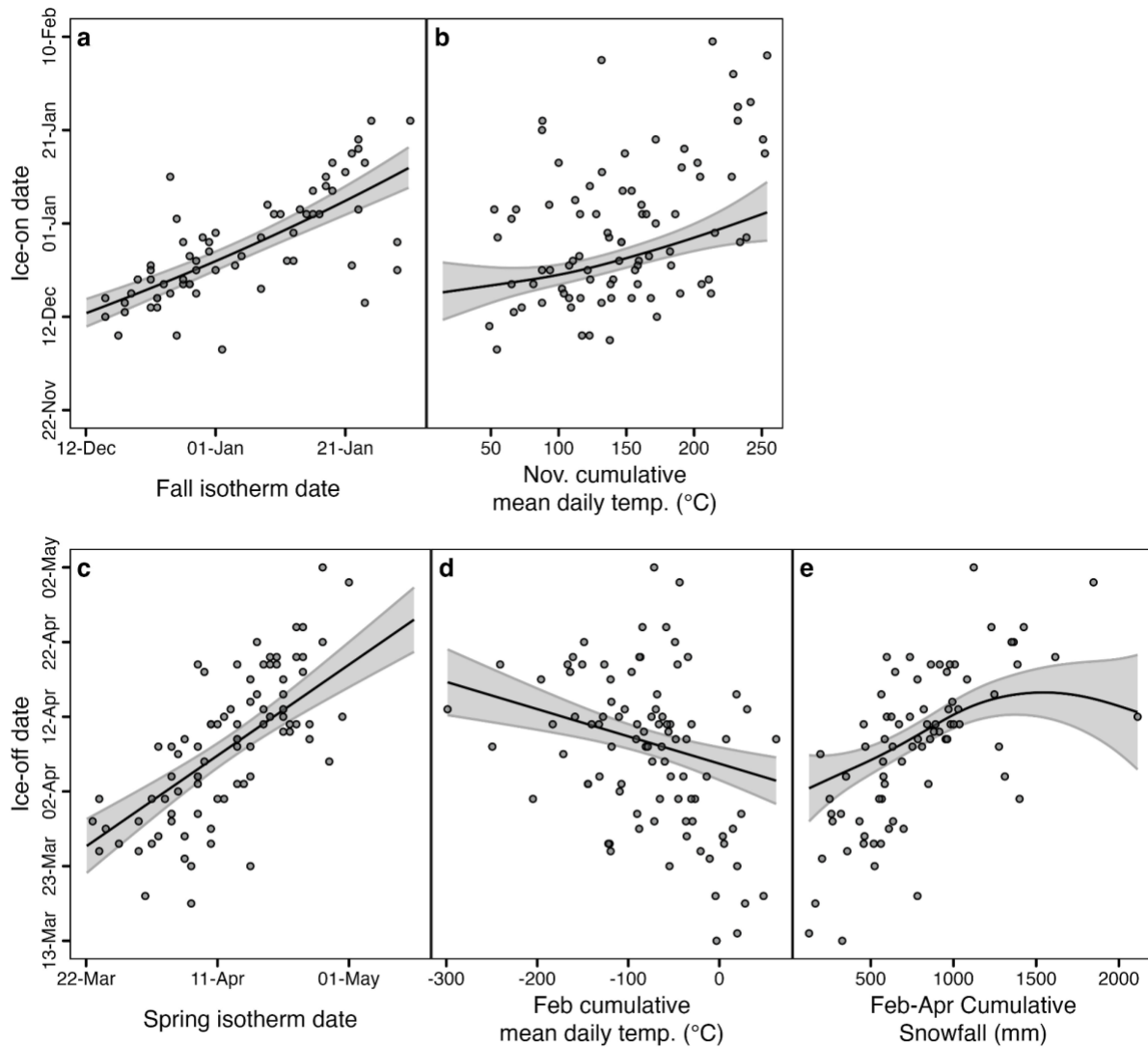


Figure 3. General Additive Model results for ice-on date and ice-off date. Ice-on date was best explained by (a) 17 days after that the maximum daily air temperature fell below the 0°C air temperature isotherm and (b) cumulative mean daily air temperature in November (deviance explained 67.5%). Ice-off date was best explained by (c) 29 days after the average daily air temperature exceeded the 4°C isotherm in the spring, (d) cumulative mean daily temperatures in February, and (e) cumulative snowfall between February and April (deviance explained 81.3%). For all panels, the points represent raw data, and the fitted curves are the predictions holding all other covariates at their median value.

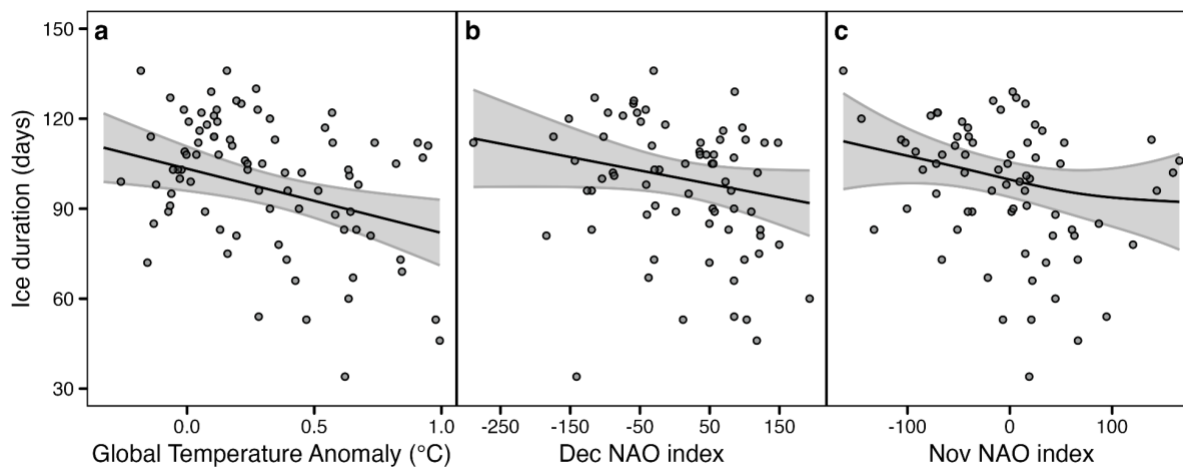


Figure 4. General Additive Model results for global drivers of ice duration. Ice duration was best explained by (a) global temperature anomaly, (b) December NAO index, and (c) November NAO index (deviance explained 24%). For all panels, the points represent raw data, and the fitted curves are the predictions holding all other covariates at their median value.

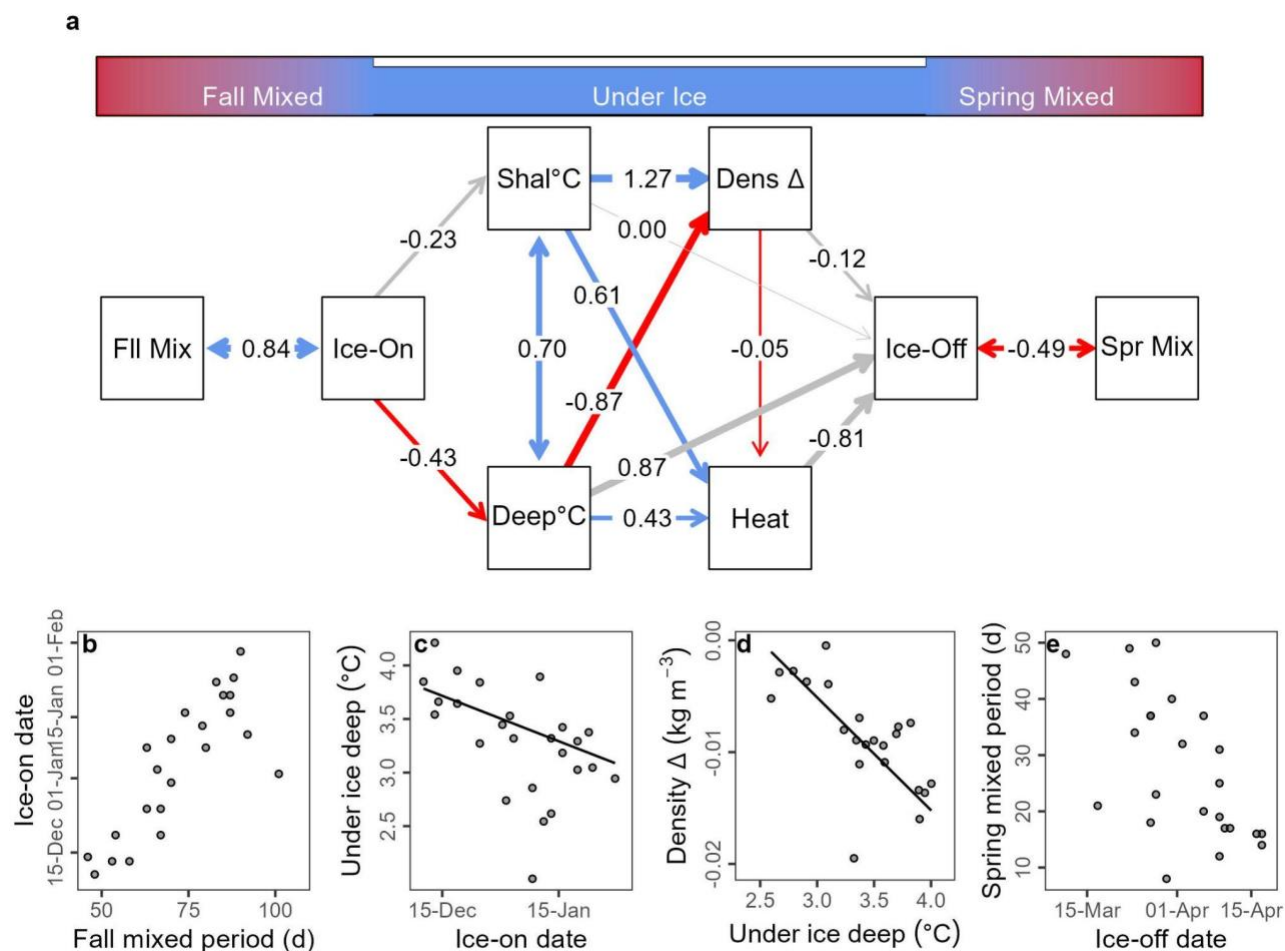


Figure 5. (a) A network plot is showing structural equation model results linking Mohonk Lake's fall-mixed, under-ice, and spring-mixed seasons via ice phenology (Ice-On and Ice-Off dates). Starting with the length of fall mixing (Fall Mix) to under-ice shallow (1-3 m: Shal°C) and deep (10-12 m: Deep°C) water temperatures, the water density difference between 1m and 11m deep (Dens Δ), and mean under-ice heat content (Heat) through the length of the spring mixing period (Spr Mix). Path coefficients are labeled on all edges with red lines indicating a significant negative relationship, blue lines indicating a significant positive relationship, grey lines indicating non-significant relationships, and the thickness of the edge arrow representing the strength of the relationship between mean-centered and unit-variance scaled variables. Single-ended arrows indicate a causal regression while double-ended arrows indicate covariance. From the structural equation model, covariance or partial residual plots for back-transformed variables are displayed for four selected significant relationships including (b) the length of the fall mixing period and ice-on date, (c) ice-on date and deep under ice water temperatures, (d) deep under ice water temperatures and water density difference between 1m and 11m deep and shallow under ice water temperatures, and (e) the length of the spring mixing period and ice-off date. For causal regression relationships, component and component plus residual were plotted as a black line to show where the fitted regression line falls. With significant covariance relationships, no regression lines were plotted.

Acknowledgments

We acknowledge, with respect, that Mohonk Lake is located on the traditional and ancestral homelands of the Munsee Lenape peoples. We thank the original data collectors including Daniel Smiley, Paul Huth, John Thompson, Christy Belardo, Natalie Feldsine, Megan Napoli, Elizabeth Long, and the Mohonk Preserve's Climate Trackers citizen science program. The Mohonk Preserve and Mohonk Mountain House were integral in facilitating long-term monitoring. IAO was supported by National Science Foundation award EPS-2019528. DCR was supported by National Science Foundation award DEB-1638575. We are grateful to Kyle Christianson, Linnea Rock, Carolina Barbosa, Benjamin Tumolo, and two anonymous reviewers for helpful feedback on earlier versions of this manuscript.

Author contribution statement:

IAO and DCR co-led the entire manuscript effort, developed the research questions, designed the study approach, wrote the paper, and contributed equally. IAO conducted the trend and generalized additive model analyses. DCR conducted the structural equation model analyses.

References

- Adrian, R., Walz, N., Hintze, T., Hoeg, S., & Rusche, R. (1999). Effects of ice duration on plankton succession during spring in a shallow polymictic lake. *Freshwater Biology*, 41(3), 621–634.
- Bai, X., Wang, J., Sellinger, C., Clites, A., & Assel, R. (2012). Interannual variability of Great Lakes ice cover and its relationship to NAO and ENSO. *Journal of Geophysical Research: Oceans*, 117(C3). <https://doi.org/10.1029/2010JC006932>
- Benson, B. J., Magnuson, J. J., Jensen, O. P., Card, V. M., Hodgkins, G., Korhonen, J., Livingstone, D. M., Stewart, K. M., Weyhenmeyer, G. A., & Granin, N. G. (2012).

- Extreme events, trends, and variability in Northern Hemisphere lake-ice phenology (1855–2005). *Climatic Change*, 112(2), 299–323. <https://doi.org/10.1007/s10584-011-0212-8>
- Beyene, M. T., & Jain, S. (2015). Wintertime weather-climate variability and its links to early spring ice-out in Maine lakes. *Limnology and Oceanography*, 60(6), 1890–1905.
- Bollinger, J. (1992). Using bollinger bands. *Stocks & Commodities*, 10(2), 47–51.
- Brentrup, J. A., Richardson, D. C., Carey, C. C., Ward, N. K., Bruesewitz, D. A., & Weathers, K. C. (2021). Under-ice respiration rates shift the annual carbon cycle in the mixed layer of an oligotrophic lake from autotrophy to heterotrophy. *Inland Waters*, 11(1), 114–123. <https://doi.org/10.1080/20442041.2020.1805261>
- Briatte, F. (2021). *ggnetwork: Geometries to Plot Networks with “ggplot2.”* <https://CRAN.R-project.org/package=ggnetwork>
- Bronaugh, D., & Consortium, A. W. for the P. C. I. (2019). *zyp: Zhang + Yue-Pilon Trends Package* (0.10-1.1). <https://CRAN.R-project.org/package=zyp>
- Bruesewitz, D. A., Carey, C. C., Richardson, D. C., & Weathers, K. C. (2015). Under-ice thermal stratification dynamics of a large, deep lake revealed by high-frequency data. *Limnology and Oceanography*, 60(2), 347–359. <https://doi.org/10.1002/lno.10014>
- Caldwell, T. J., Chandra, S., Albright, T. P., Harpold, A. A., Dilts, T. E., Greenberg, J. A., Sadro, S., & Dettinger, M. D. (2021). Drivers and projections of ice phenology in mountain lakes in the western United States. *Limnology and Oceanography*, 66(3), 995–1008. <https://doi.org/10.1002/lno.11656>
- Cavaliere, E., Fournier, I. B., Hazuková, V., Rue, G. P., Sadro, S., Berger, S. A., Cotner, J. B., Dugan, H. A., Hampton, S. E., Lottig, N. R., McMeans, B. C., Ozersky, T., Powers, S. M., Rautio, M., & O’Reilly, C. M. (2021). The Lake Ice Continuum Concept: Influence of Winter Conditions on Energy and Ecosystem Dynamics. *Journal of Geophysical Research: Biogeosciences*, 126(11), 1–20. <https://doi.org/10.1029/2020JG006165>

- Christianson, K. R., Loria, K. A., Blanken, P. D., Caine, N., & Johnson, P. T. J. (2021). On thin ice: Linking elevation and long-term losses of lake ice cover. *Limnology and Oceanography Letters*, 6(2), 77–84. <https://doi.org/10.1002/lol2.10181>
- Dokulil, M. T., Jagsch, A., George, G. D., Anneville, O., Jankowski, T., Wahl, B., Lenhart, B., Blenckner, T., & Teubner, K. (2006). Twenty years of spatially coherent deepwater warming in lakes across Europe related to the North Atlantic Oscillation. *Limnology and Oceanography*, 51(6), 2787–2793.
- Dugan, H. A. (2021). A Comparison of Ecological Memory of Lake Ice-Off in Eight North-Temperate Lakes. *Journal of Geophysical Research: Biogeosciences*, 126(6), 1–13. <https://doi.org/10.1029/2020jg006232>
- Epskamp, S. (2022). *semPlot: Path Diagrams and Visual Analysis of Various SEM Packages' Output*. <https://CRAN.R-project.org/package=semPlot>
- Grace, J. B., Anderson, T. M., Olf, H., & Scheiner, S. M. (2010). On the specification of structural equation models for ecological systems. *Ecological Monographs*, 80(1), 67–87.
- Hastie, T., & Tibshirani, R. (1987). *Generalized Additive Models, Cubic Splines and Personalized Likelihood*. University of Toronto, Department of Statistics.
- Hébert, M.-P., Beisner, B. E., Rautio, M., & Fussmann, G. F. (2021). Warming winters in lakes: Later ice onset promotes consumer overwintering and shapes springtime planktonic food webs. *Proceedings of the National Academy of Sciences*, 118(48). <https://doi.org/10.1073/PNAS.2114840118>
- Higgins, S. N., Desjardins, C. M., Drouin, H., Hrenchuk, L. E., & van der Sanden, J. J. (2021). The Role of Climate and Lake Size in Regulating the Ice Phenology of Boreal Lakes. *Journal of Geophysical Research: Biogeosciences*, 126(3), 1–11. <https://doi.org/10.1029/2020JG005898>
- Hrycik, A. R., McFarland, S., Morales-Williams, A., & Stockwell, J. D. (2022). Winter severity
- Oleksy & Richardson*

- shapes spring plankton succession in a small, eutrophic lake. *Hydrobiologia*, 849(9), 2127–2144. <https://doi.org/10.1007/s10750-022-04854-4>
- Jansen, J., MacIntyre, S., Barrett, D. C., Chin, Y.-P., Cortés, A., Forrest, A. L., Hrycik, A. R., Martin, R., McMeans, B. C., Rautio, M., & Schwefel, R. (2021). Winter Limnology: How do Hydrodynamics and Biogeochemistry Shape Ecosystems Under Ice? *Journal of Geophysical Research: Biogeosciences*, 126(6), e2020JG006237. <https://doi.org/10.1029/2020JG006237>
- Kainz, M. J., Ptacnik, R., Rasconi, S., & Hager, H. H. (2017). Irregular changes in lake surface water temperature and ice cover in subalpine Lake Lunz, Austria. *Inland Waters*, 7(1), 27–33. <https://doi.org/10.1080/20442041.2017.1294332>
- Kirillin, G., Leppäranta, M., Terzhevik, A., Granin, N., Bernhardt, J., Engelhardt, C., Efremova, T., Golosov, S., Palshin, N., Sherstyankin, P., Zdrovennova, G., & Zdrovennov, R. (2012). Physics of seasonally ice-covered lakes: A review. *Aquatic Sciences*, 74(4), 659–682. <https://doi.org/10.1007/s00027-012-0279-y>
- Kouraev, A. V., Semovski, S. V., Shimaraev, M. N., Mognard, N. M., Legrésy, B., & Rémy, F. (2007). The ice regime of Lake Baikal from historical and satellite data: Relationship to air temperature, dynamical, and other factors. *Limnology and Oceanography*, 52(3), 1268–1286. <https://doi.org/10.4319/lo.2007.52.3.1268>
- Li, X., Peng, S., Xi, Y., Woolway, R. I., & Liu, G. (2022). Earlier ice loss accelerates lake warming in the Northern Hemisphere. *Nature Communications*, 13(1), Article 1. <https://doi.org/10.1038/s41467-022-32830-y>
- Magnuson, J. J., Wynne, R. H., Benson, B. J., & Robertson, D. M. (2000). Lake and river ice as a powerful indicator of past and present climates. *SIL Proceedings, 1922-2010*, 27(5), 2749–2756. <https://doi.org/10.1080/03680770.1998.11898166>
- National Weather Service. (2020). *Climate Prediction Center—Teleconnections: North Atlantic Oscillation*. <https://www.cpc.ncep.noaa.gov/products/precip/CWlink/pna/nao.shtml>

- NOAA. (2020). *Global Surface Temperature Anomalies | Monitoring References | National Centers for Environmental Information (NCEI)*. <https://www.ncdc.noaa.gov/monitoring-references/faq/anomalies.php#anomalies>
- Oleksy, I. A., & Richardson, D. C. (2021). Climate Change and Teleconnections Amplify Lake Stratification With Differential Local Controls of Surface Water Warming and Deep Water Cooling. *Geophysical Research Letters*, *48*(5), 1–11.
<https://doi.org/10.1029/2020GL090959>
- Pedersen, T. L. (2022). *patchwork: The Composer of Plots*. <https://CRAN.R-project.org/package=patchwork>
- Pohlert, T. (2020). *trend: Non-Parametric Trend Tests and Change-Point Detection (1.1.2)*. <https://CRAN.R-project.org/package=trend>
- Preston, D. L., Caine, N., McKnight, D. M., Williams, M. W., Hell, K., Miller, M. P., Hart, S. J., & Johnson, P. T. J. (2016). Climate regulates alpine lake ice cover phenology and aquatic ecosystem structure. *Geophysical Research Letters*, *43*(10), 5353–5360.
<https://doi.org/10.1002/2016GL069036>
- Prowse, T., Alfredsen, K., Beltaos, S., Bonsal, B. R., Bowden, W. B., Duguay, C. R., Korhola, A., McNamara, J., Vincent, W. F., Vuglinsky, V., Walter Anthony, K. M., & Weyhenmeyer, G. A. (2011). Effects of Changes in Arctic Lake and River Ice. *AMBIO*, *40*(1), 63–74. <https://doi.org/10.1007/s13280-011-0217-6>
- R Core Team. (2022). *R: A Language and Environment for Statistical Computing*. R Foundation for Statistical Computing. <https://www.R-project.org/>
- Read, J. S., Hamilton, D. P., Desai, A. R., Rose, K. C., MacIntyre, S., Lenters, J. D., Smyth, R. L., Hanson, P. C., Cole, J. J., Staehr, P. A., Rusak, J. A., Pierson, D. C., Brookes, J. D., Laas, A., & Wu, C. H. (2012). Lake-size dependency of wind shear and convection as controls on gas exchange. *Geophysical Research Letters*, *39*(9).
<https://doi.org/10.1029/2012GL051886>

- Richardson, D. C., Charifson, D. M., Davis, B. A., Farragher, M. J., Krebs, B. S., Long, E. C., Napoli, M., & Wilcove, B. A. (2018). Watershed management and underlying geology in three lakes control divergent responses to decreasing acid precipitation. *Inland Waters*, 8(1), 70–81. <https://doi.org/10.1080/20442041.2018.1428428>
- Robertson, D. M., Ragotzkie, R. A., & Magnuson, J. J. (1992). Lake ice records used to detect historical and future climatic changes. *Climatic Change*, 21(4), 407–427. <https://doi.org/10.1007/BF00141379>
- Rosseel, Y. (2012). lavaan: An R Package for Structural Equation Modeling. In *Journal of Statistical Software* (Vol. 48). <https://doi.org/10.18637/jss.v048.i02>
- Salonen, K., Leppäranta, M., Viljanen, M., & Gulati, R. D. (2009). Perspectives in winter limnology: Closing the annual cycle of freezing lakes. *Aquatic Ecology*, 43(3), 609–616. <https://doi.org/10.1007/s10452-009-9278-z>
- Sharma, S., Blagrove, K., Magnuson, J. J., O'Reilly, C. M., Oliver, S., Batt, R. D., Magee, M. R., Straile, D., Weyhenmeyer, G. A., Winslow, L., & Woolway, R. I. (2019). Widespread loss of lake ice around the Northern Hemisphere in a warming world. *Nature Climate Change*, 9(3), Article 3. <https://doi.org/10.1038/s41558-018-0393-5>
- Sharma, S., Filazzola, A., Nguyen, T., Imrit, M. A., Blagrove, K., Bouffard, D., Daly, J., Feldman, H., Feldsine, N., Hendricks-Franssen, H.-J., Granin, N., Hecock, R., L'Abée-Lund, J. H., Hopkins, E., Howk, N., Iacono, M., Knoll, L. B., Korhonen, J., Malmquist, H. J., ... Magnuson, J. J. (2022). Long-term ice phenology records spanning up to 578 years for 78 lakes around the Northern Hemisphere. *Scientific Data*, 9(1), Article 1. <https://doi.org/10.1038/s41597-022-01391-6>
- Sharma, S., & Magnuson, J. J. (2014). Oscillatory dynamics do not mask linear trends in the timing of ice breakup for Northern Hemisphere lakes from 1855 to 2004. *Climatic Change*, 124(4), 835–847. <https://doi.org/10.1007/s10584-014-1125-0>
- Sharma, S., Magnuson, J. J., Mendoza, G., & Carpenter, S. R. (2013). Influences of local
- Oleksy & Richardson*

- weather, large-scale climatic drivers, and the ca. 11 year solar cycle on lake ice breakup dates; 1905–2004. *Climatic Change*, 118(3), 857–870. <https://doi.org/10.1007/s10584-012-0670-7>
- Sharma, S., Richardson, D. C., Woolway, R. I., Imrit, M. A., Bouffard, D., Blagrove, K., Daly, J., Filazzola, A., Granin, N., Korhonen, J., Magnuson, J., Marszelewski, W., Matsuzaki, S.-I. S., Perry, W., Robertson, D. M., Rudstam, L. G., Weyhenmeyer, G. A., & Yao, H. (2021). Loss of Ice Cover, Shifting Phenology, and More Extreme Events in Northern Hemisphere Lakes. *Journal of Geophysical Research: Biogeosciences*, 126(10), e2021JG006348. <https://doi.org/10.1029/2021JG006348>
- Smits, A. P., Gomez, N. W., Dozier, J., & Sadro, S. (2021). Winter Climate and Lake Morphology Control Ice Phenology and Under-Ice Temperature and Oxygen Regimes in Mountain Lakes. *Journal of Geophysical Research: Biogeosciences*, 126(8), e2021JG006277. <https://doi.org/10.1029/2021JG006277>
- Smits, A. P., Macintyre, S., & Sadro, S. (2020). Snowpack determines relative importance of climate factors driving summer lake warming. *Limnology and Oceanography Letters*, 5(3), Article 3. <https://doi.org/10.1002/lol2.10147>
- Wetzel, R. G., Likens, G. E., Wetzel, R. G., & Likens, G. E. (2000). The heat budget of lakes. *Limnological Analyses*, 45–56.
- Wickham, H. (2016). *ggplot2: Elegant Graphics for Data Analysis*. Springer-Verlag New York. <https://ggplot2.tidyverse.org>
- Wilke, C. O. (2020). *cowplot: Streamlined Plot Theme and Plot Annotations for “ggplot2.”* <https://CRAN.R-project.org/package=cowplot>
- Wilkinson, G. M., Walter, J., Fleck, R., & Pace, M. L. (2020). Beyond the trends: The need to understand multiannual dynamics in aquatic ecosystems. *Limnology and Oceanography Letters*, lol2.10153. <https://doi.org/10.1002/lol2.10153>
- Wood, F. S. (1973). The Use of Individual Effects and Residuals in Fitting Equations to Data. *Oleksy & Richardson*

- Technometrics*, 15(4), 677–695. <https://doi.org/10.1080/00401706.1973.10489104>
- Wood, S. (2019). *mgcv: Mixed GAM Computation Vehicle with Automatic Smoothness Estimation* (1.8-31). <https://CRAN.R-project.org/package=mgcv>
- Wood, S. N. (2017). *Generalized Additive Models* (2nd ed.). New York: Chapman and Hall/CRC.
- Woolway, R. I., Denfeld, B., Tan, Z., Jansen, J., Weyhenmeyer, G. A., & La Fuente, S. (2022). Winter inverse lake stratification under historic and future climate change. *Limnology and Oceanography Letters*, 7(4), 302–311. <https://doi.org/10.1002/lol2.10231>
- Woolway, R. I., Sharma, S., & Smol, J. P. (2022). Lakes in Hot Water: The Impacts of a Changing Climate on Aquatic Ecosystems. *BioScience*, 72(11), 1050–1061. <https://doi.org/10.1093/biosci/biac052>
- Yang, B., Wells, M. G., McMeans, B. C., Dugan, H. A., Rusak, J. A., Weyhenmeyer, G. A., Brenttrup, J. A., Hrycik, A. R., Laas, A., Pilla, R. M., Austin, J. A., Blanchfield, P. J., Carey, C. C., Guzzo, M. M., Lottig, N. R., MacKay, M. D., Middel, T. A., Pierson, D. C., Wang, J., & Young, J. D. (2021). A New Thermal Categorization of Ice-Covered Lakes. *Geophysical Research Letters*, 48(3). <https://doi.org/10.1029/2020GL091374>
- Yang, B., Young, J., Brown, L., & Wells, M. (2017). High-Frequency Observations of Temperature and Dissolved Oxygen Reveal Under-Ice Convection in a Large Lake. *Geophysical Research Letters*, 44(24), 12,218–12,226. <https://doi.org/10.1002/2017GL075373>
- Yu, G. (2021). *ggplotify: Convert Plot to “grob” or “ggplot” Object*. <https://CRAN.R-project.org/package=ggplotify>

Supplemental text.

Sequential standard deviation windows: To assess changing variability of ice phenology, we evaluated 3 to 13-year windows of ice-on, ice-off, and ice duration for sequential windows as follows. First, we identified Y different series of standard deviations (Y years where $Y=3, \dots, 13$) starting with 1932 through 1932+ $Y-1$, beyond which the windows would repeat. Next, for each series, we calculated the standard deviation for sequential windows of Y years. For example, there are four unique versions of the 4-year windows (Fig. S1), nine unique versions of the 9-year windows (Fig. S2), and 13 unique versions of the 13-year windows (Fig. S3). For the 4-year sequential windows, the first version would start in 1932 with standard deviations calculated for 4-year sequential windows: 1932-1936, 1937-1941, etc..., the second version would start in 1933: 1933-1937, 1938-1942, etc... To determine if variability is increasing for each window size, we calculated the Theil-Sens slope and intercept. Ultimately, shorter windows had the most sequential standard deviation windows possible but the least number of unique versions. The 13-year window had only 5 or 6 different sequential standard deviation calculations but the most unique versions. To balance these two factors, we used 9-year windows for both analyses.

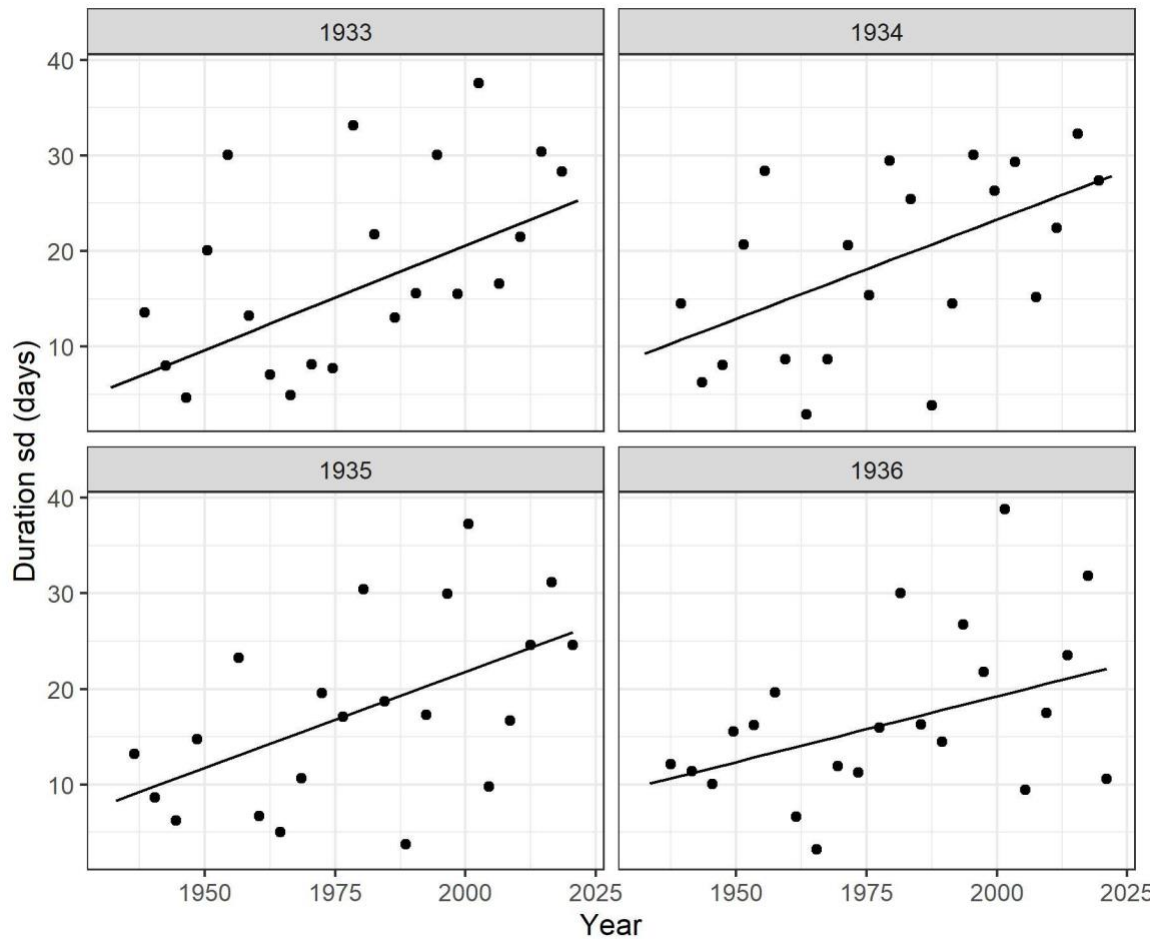


Figure S1. Standard deviations for all possible 4-year sequential windows where the year in each panel's title indicates the start year of the first segment. Additional sequential windows would overlap existing windows. The line indicates the Theil-Sen slope for each sequence of standard deviations.

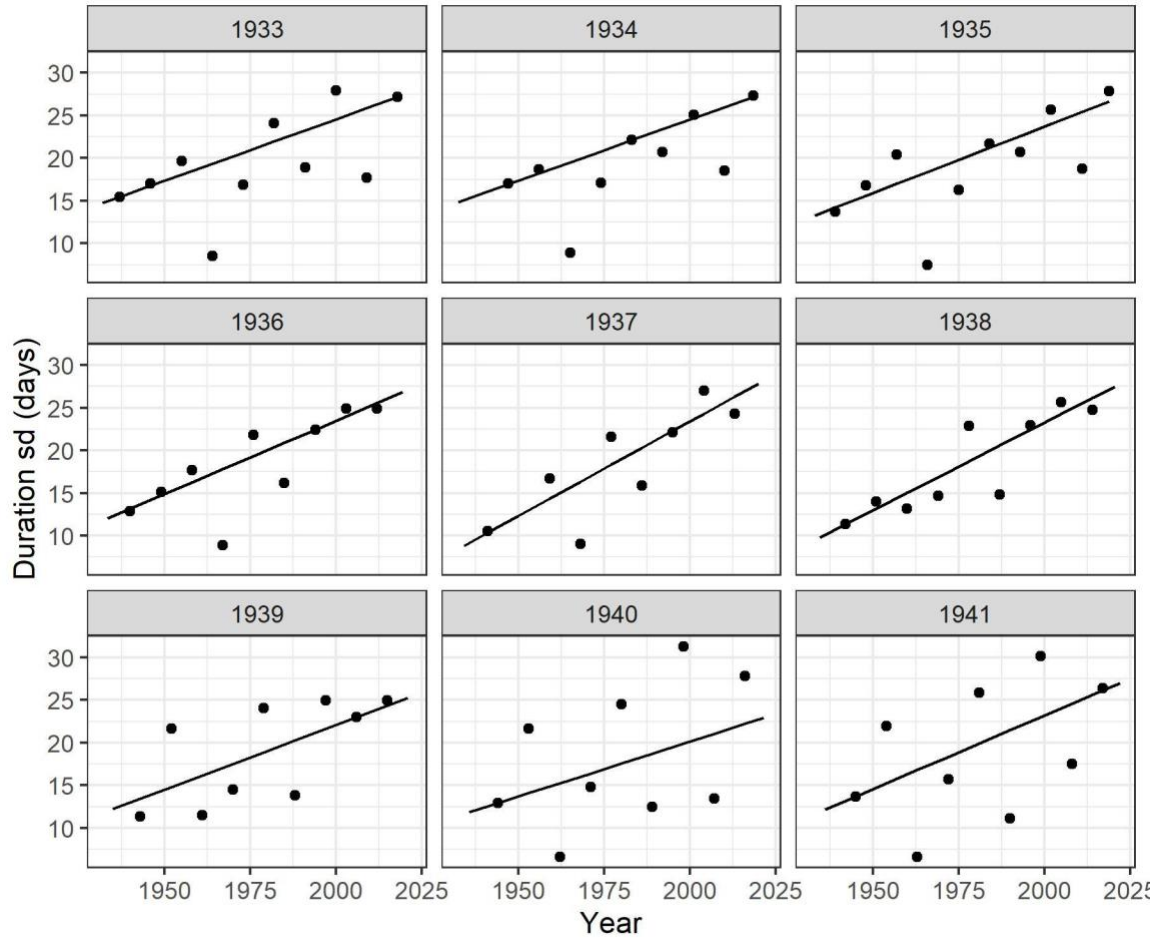


Figure S2. Standard deviations for all possible 9-year sequential windows where the year in each panel's title indicates the start year of the first segment. Additional sequential windows would overlap existing windows. The line indicates the Theil-Sen slope for each sequence of standard deviations.

Changing under-ice thermodynamics

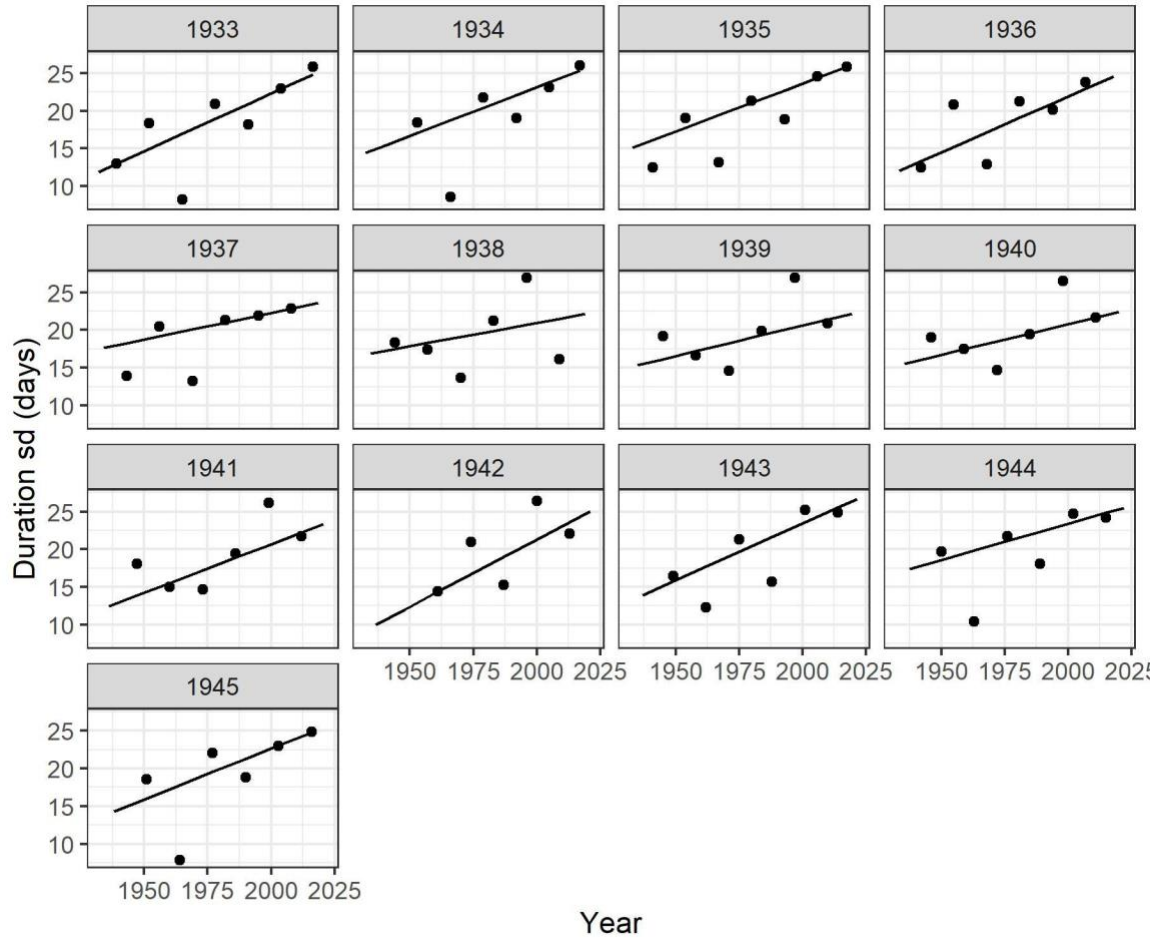


Figure S3. Standard deviations for all possible 13-year sequential windows where the year in each panel's title indicates the start year of the first segment. Additional sequential windows would overlap existing windows. The line indicates the Theil-Sen slope for each sequence of standard deviations.

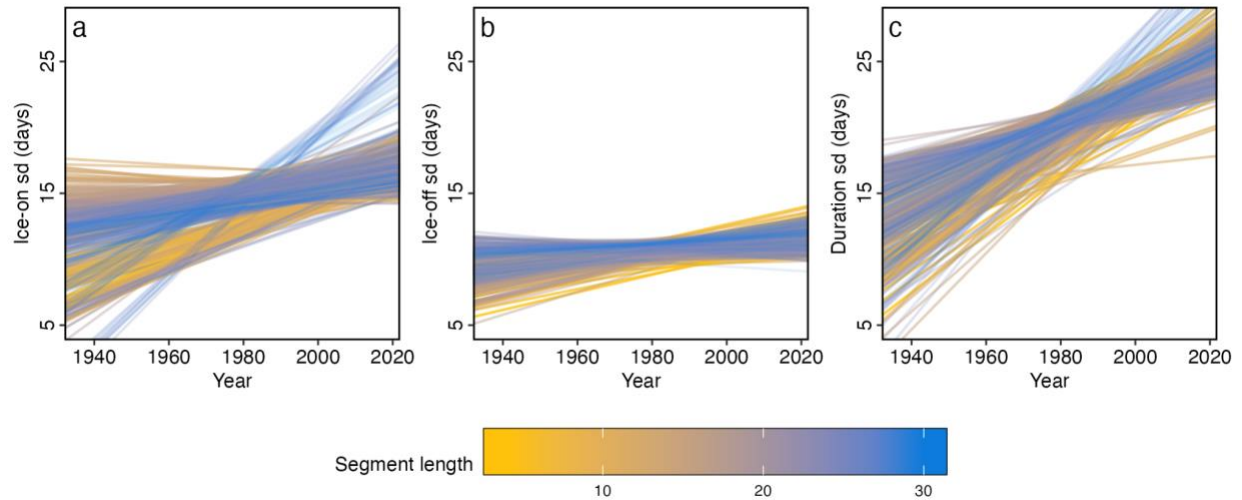


Figure S4. Theil-Sen slope fits for (a) ice-on standard deviation (sd), (b) ice-off sd, and (c) duration sd compared across years of record (1931-2022). Sds were calculated from sequential windows of time across 4 to 30 years with color representing the sequential window length (segment length). For example, four year windows had four unique slopes (see Figure S1), 13-year sequential windows had 13 different slopes (see Figure S3), and 30 year windows had 30 different slopes. Overall, this resulted in 459 total best-fit lines in each panel.

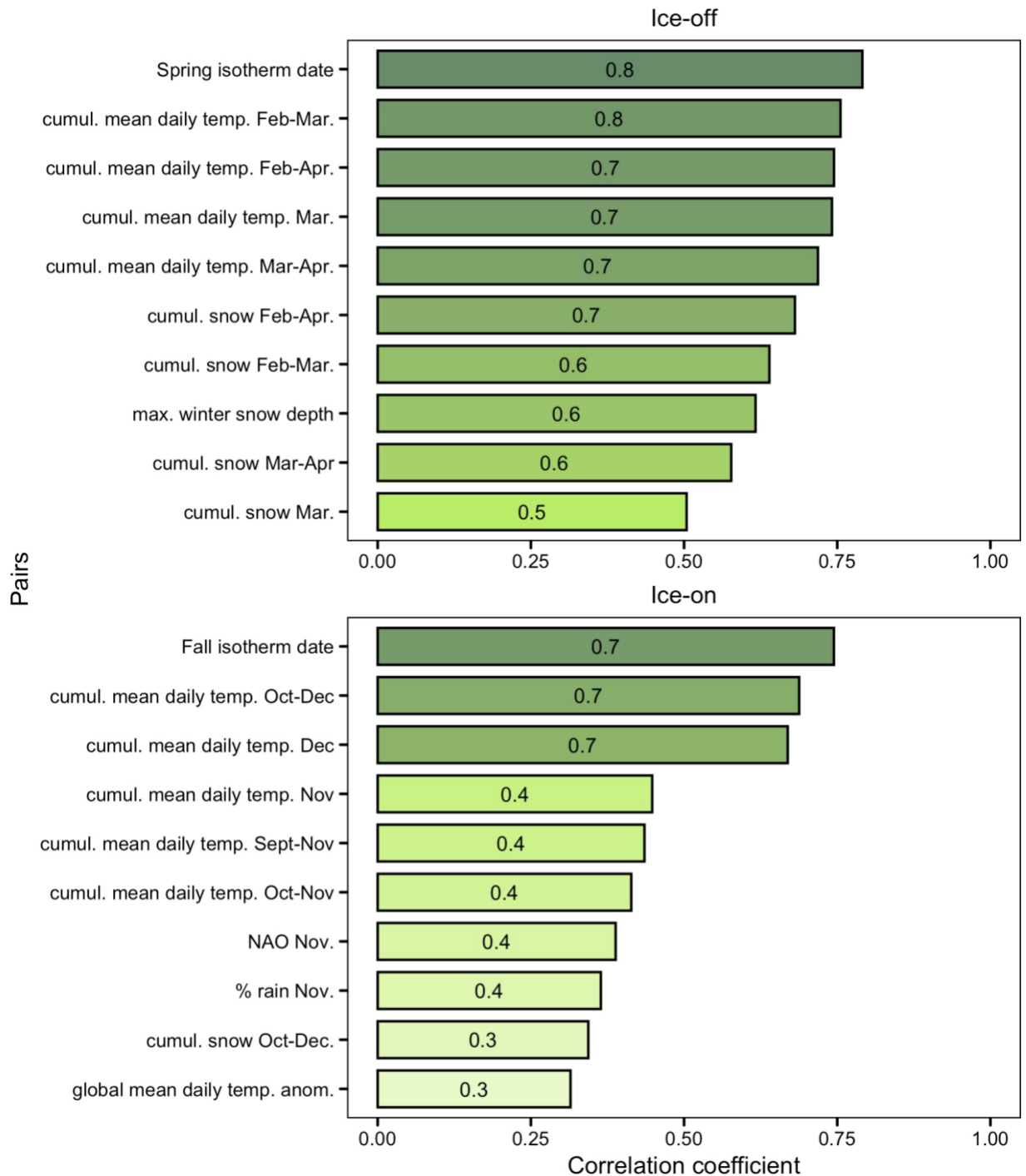


Figure S5. Pairwise correlation (Pearson’s r) between ice-off (top panel) and ice-on (bottom panel) and variation meteorological variables ranked in order from strongest to weakest.

Prior to building the models, we tested for collinearity among the variables. For collinear pairs with correlation $>|0.7|$, we chose the variable with the higher correlation strength with ice-on or ice-off date.

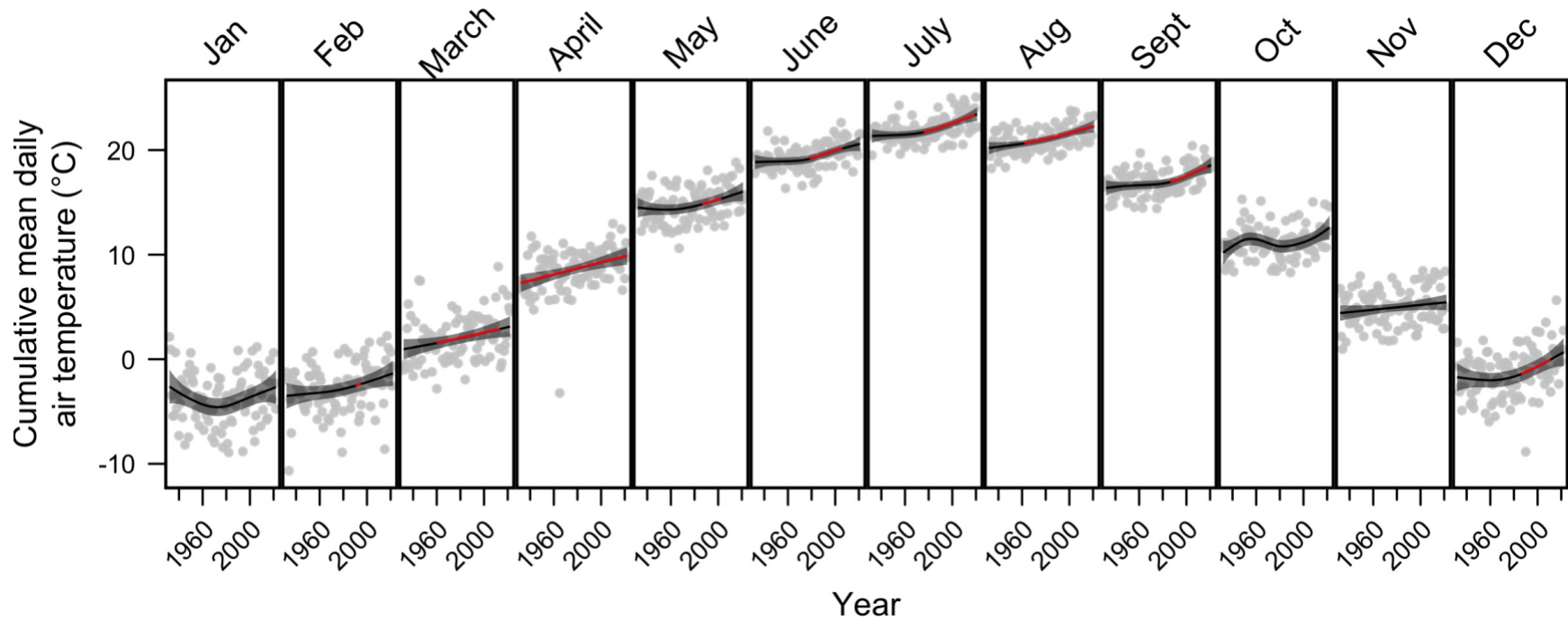


Figure S6. Cumulative mean daily air temperatures at Mohonk Lake between 1932 and 2022. Grey points are raw data and lines are a fitted trend. Shading around trend shows 95% confidence intervals. Red lines indicate periods of a significant temperature increase as indicated by the first derivative of the generalized additive model.

Table S1. List of top 3 GAMs fitted to ice-on and ice-off date. Model complexity (EDF; effective degrees of freedom) and AIC scores are shown for each model. The models highlighted in the text are ranked #1 and model summaries are contained in supplemental Table S2.

Response	Predictors	EDF	AIC	Rank	% Dev. explained
Ice on date	Fall isotherm date, Cumulative mean daily temp. Nov.	3.6	461.8	1	67.7%
Ice on date	Fall isotherm date	2.0	478.9	2	56.4%
Ice on date	Cumulative mean daily air temp. Nov, Cumulative mean daily air temp. Dec	3.0	633.3	3	53.3%
Ice off date	Cumulative mean daily air temp. February, Spring isotherm date, Cumulative snowfall Feb.-Apr., Ice in day of year	6.9	505.3	1	81.8%
Ice off date	Cumulative mean daily air temp. February, Spring isotherm date, Cumulative snowfall Feb.-Apr.	6.5	516.3	2	80.4%
Ice off date	Cumulative mean daily temp. Feb.-Mar., Cumulative snowfall Feb.-Apr., Ice in day of year	8.5	523.7	3	78.2%

Table S2. Top ranking model summary for ice on date and ice off date.

		Estimate	Est. df.	Ref. df	Chi.sq	F	p-value
Ice duration	Intercept	97.6					
	Global temperature anomaly		1.0	1.0	8.2	-	0.0042
	NAO index Nov.		1.4	1.8	4.1	-	0.1387
	NAO index Dec.		1.0	1.0	3.1	-	0.0764
Ice-on date	Intercept	4.4					
	Fall isotherm date		1.0	1.0	-	110.4	< 0.001
	Cumulative mean daily temp. Nov.		1.5	1.9	-	11.8	< 0.001
Ice-off date	Intercept	95.38					
	Cumulative mean daily temp. Feb.		1.0	1.0	-	15.3	< 0.001
	Spring isotherm date		1.0	1.0	-	83.4	< 0.001
	Cumulative snow Feb-Apr.		2.9	3.6	-	8.9	< 0.001
	Ice-on day of year		1.0	1.0	-	1.9	0.16

Table S3. Sens slopes on all the computed climatic variables for Mohonk Lake. We computed Sens slopes for all monthly and seasonal ENSO and NAO variables, but all Sens slope p-values were > 0.05 and therefore not printed in this table.

*** p < 0.001; ** p < 0.01; * p < 0.05.

Climatic variable	p-value	Slope	Intercept	z-statistic
Global temp. anomaly (°C)	<0.001***	0.0112	-21.8	9.93
Date of maximum snowfall	0.8183	0.167	-186	0.23
Maximum snow depth (mm)	0.7162	-2.21	4.87e+03	-0.363
Sept. cumulative snow (mm)	1	0	0	0
Sept.-Nov. cumulative rain (mm)	0.114	0.865	-1.4e+03	1.58
Sept.-Nov. number of days mean daily air T below zero	0.0558	-0.0213	46.3	-1.91
Sept.-Nov. number of days min daily air T below zero	0.18	-0.0286	69.9	-1.34
Sept.-Oct. number of days mean daily air T below zero	0.0311*	0	0	-2.16
Sept.-Oct. number of days min daily air T below zero	0.2535	0	1.5	-1.14
Sept. % of precipitation as rain	1	0	100	0
Sept. number of days min daily air T below zero	1	0	0	0
Sept.-Nov. cumulative mean daily air temp. (°C)	0.0011**	1.34	-1.64e+03	3.27
Sept.-Nov. cumulative snow (mm)	0.2629	-0.0577	171	-1.12
Sept.-Oct. cumulative mean daily air temp. (°C)	0.0006***	0.972	-1.06e+03	3.41

Changing under-ice thermodynamics

Climatic variable	p-value	Slope	Intercept	z-statistic
Sept.-Oct. cumulative rain (mm)	0.0203*	0.977	-1.73e+03	2.32
Sept.-Oct. cumulative snow (mm)	0.272	0	0	1.1
Sept. cumulative mean daily air temp. (°C)	0.0001***	0.644	-760	3.9
Sept. cumulative rain (mm)	0.2184	0.371	-631	1.23
Sept. number of days mean daily air T below zero	1	0	0	0
Oct cumulative mean daily air temp. (°C)	0.1013	0.317	-282	1.64
Oct number of days mean daily air T below zero	0.0203*	0	0	-2.32
Oct.-Dec cumulative mean daily air temp. (°C)	0.0033**	1.41	-2.34e+03	2.93
Oct.-Dec. cumulative rain (mm)	0.0287*	0.813	-1.3e+03	2.19
Oct.-Dec. cumulative snow (mm)	0.399	0.798	-1.21e+03	0.843
Oct.-Dec. number of days mean daily air T below zero	0.0025**	-0.0882	198	-3.02
Oct.-Dec. number of days min daily air T below zero	0.0574	-0.0519	143	-1.9
Oct.-Nov cumulative mean daily air temp. (°C)	0.0365*	0.675	-839	2.09
Oct.-Nov. cumulative rain (mm)	0.0435*	0.539	-857	2.02
Oct.-Nov. number of days mean daily air T below zero	0.0511	-0.0204	44.7	-1.95
Oct.-Nov. number of days min daily air T below zero	0.1596	-0.0286	69.8	-1.41

Climatic variable	p-value	Slope	Intercept	z-statistic
Oct. % of precipitation as rain	0.282	0	100	-1.08
Oct. cumulative rain (mm)	0.0065**	0.629	-1.15e+03	2.72
Oct. cumulative snow (mm)	0.2791	0	0	1.08
Oct. number of days min daily air T below zero	0.1721	0	1	-1.37
Oct.-Nov. cumulative snow (mm)	0.1781	-0.127	304	-1.35
Nov cumulative mean daily air temp. (°C)	0.2223	0.302	-451	1.22
Nov. % of precipitation as rain	0.0396*	0.0934	-115	2.06
Nov. cumulative rain (mm)	0.4715	-0.136	369	-0.72
Nov. cumulative snow (mm)	0.0551	-0.141	329	-1.92
Nov. number of days mean daily air T below zero	0.0709	-0.0189	41.6	-1.81
Nov. number of days min daily air T below zero	0.3221	-0.0182	48.1	-0.99
Dec. % of precipitation as rain	1	0	26.7	0
Dec. cumulative rain (mm)	0.0735	0.321	-530	1.79
Dec. cumulative snow (mm)	0.2248	1.12	-1.94e+03	1.21
Fall isotherm date	0.02*	0.214	-330	2.25
Dec. number of days mean daily air T below zero	0.0181*	-0.0588	134	-2.36

Climatic variable	p-value	Slope	Intercept	z-statistic
Dec. number of days min daily air T below zero	0.176	-0.0196	64.2	-1.35
Dec. cumulative mean daily air temp. (°C)	0.0046**	0.78	-1.58e+03	2.84
Jan cumulative rain (mm)	0.9045	0.0201	41.5	0.12
Jan-Mar cumulative mean daily air temp. (°C)	0.0183*	1.39	-2.9e+03	2.36
Jan-Mar. cumulative rain (mm)	0.3423	0.326	-378	0.95
Jan-Mar. cumulative snow (mm)	0.8747	-0.207	1.41e+03	-0.158
Jan. % of precipitation as rain	0.959	0.0015	18.1	0.0514
Jan. cumulative mean daily air temp. (°C)	0.624	0.198	-513	0.49
Jan. cumulative snow (mm)	0.9317	0	343	-0.0857
Jan. number of days mean daily air T below zero	0.6182	0	24	-0.498
Jan. number of days min daily air T below zero	0.1583	0	29	-1.41
Feb cumulative mean daily air temp. (°C)	0.0268*	0.599	-1.26e+03	2.21
Feb-Apr. cumulative mean daily air temp. (°C)	0.0001***	2.34	-4.39e+03	4.03
Feb-Apr. cumulative rain (mm)	0.6143	0.155	-36.7	0.504
Feb-Apr. cumulative snow (mm)	0.6858	-0.714	2.12e+03	-0.405
Feb-Mar cumulative mean daily air temp. (°C)	0.0021**	1.43	-2.85e+03	3.07

Climatic variable	p-value	Slope	Intercept	z-statistic
Feb-Mar. cumulative rain (mm)	0.6264	0.121	-62.6	0.487
Feb-Mar. cumulative snow (mm)	0.8855	-0.186	1.01e+03	-0.144
Feb-Mar. number of days mean daily air T above zero	0.0011**	0.0968	-162	3.27
Feb-Mar. number of days min daily air T above zero	0.0003***	0.087	-161	3.63
Feb. % of precipitation as rain	0.6708	0.016	-13.7	0.425
Feb. cumulative rain (mm)	0.5928	0.0635	-49.8	0.535
Feb. cumulative snow (mm)	0.6808	-0.341	1.01e+03	-0.411
Feb. number of days mean daily air T below zero	0.0496*	-0.037	92.7	-1.96
Feb. number of days min daily air T below zero	0.0036**	-0.0263	77.8	-2.91
Mar-Apr cumulative mean daily air temp. (°C)	0.0002***	1.59	-2.82e+03	3.79
Mar-Apr. cumulative rain (mm)	0.7865	0.0889	16.5	0.271
Mar-Apr. cumulative snow (mm)	0.2235	-0.998	2.3e+03	-1.22
Mar-Apr. number of days mean daily air T above zero	0.0029**	0.0625	-73.9	2.98
Mar-Apr. number of days min daily air T above zero	0.0007***	0.0923	-150	3.4
Mar. % of precipitation as rain	0.3528	0.0534	-79.9	0.929
Spring isotherm date	0.001***	-0.143	474	-3.24

Changing under-ice thermodynamics

Climatic variable	p-value	Slope	Intercept	z-statistic
Mar. cumulative mean daily air temp. (°C)	0.0042**	0.833	-1.59e+03	2.86
Mar. cumulative rain (mm)	0.5833	0.0939	-91.4	0.548
Mar. cumulative snow (mm)	0.5213	-0.468	1.2e+03	-0.641
Mar. number of days mean daily air T above zero	0.0032**	0.0615	-102	2.95
Mar. number of days mean daily air T below zero	0.0032**	-0.0615	133	-2.95
Mar. number of days min daily air T above zero	0.0062**	0.0545	-99.4	2.73
Mar. number of days min daily air T below zero	0.0062**	-0.0545	130	-2.73
Apr. % of precipitation as rain	0.1598	0	92.9	1.41
Apr. cumulative mean daily air temp. (°C)	0.0002***	0.84	-1.4e+03	3.69
Apr. cumulative rain (mm)	0.7112	-0.0739	249	-0.37
Apr. cumulative snow (mm)	0.1652	0	7.62	-1.39
Apr. number of days mean daily air T below zero	0.1745	0	0	-1.36
Apr. number of days min daily air T below zero	0.0034**	-0.04	85.1	-2.93

Table S4. Structural equation model fits. Relationship indicates the type of relationship (covariance or regression) for each variable with the variable (indented) below. For regression, variables indicate response variable (non-indented) and predictor variable or intercept (indented). For each relationship, an estimate of fit (Estimate), standard error of the estimate (Estimate SE), test-statistic (Z statistic) and p-value are included.

Variables	Relationship	Estimate	Estimate SE	Z statistic	p-value
Ice-on date					
Fall mixed period (d)	Covariance	0.84	0.26	3.16	0.002
Under ice shallow (°C)					
Ice-on date	Regression	-0.23	0.19	-1.20	0.229
Intercept	Regression	0.09	0.19	0.47	0.637
Under ice deep (°C)					
Ice-on date	Regression	-0.43	0.17	-2.52	0.012
Intercept	Regression	0.10	0.17	0.60	0.549
Under ice deep (°C)					
Under ice shallow (°C)	Covariance	0.70	0.22	3.26	0.001
Density Δ (kg m ⁻³)					
Under ice deep (°C)	Regression	-0.87	0.36	-2.42	0.016
Under ice shallow (°C)	Regression	1.27	0.35	3.58	<0.001
Intercept	Regression	0.01	0.16	0.03	0.974
Heat content (MJ)					
Under ice deep (°C)	Regression	0.43	0.03	14.52	<0.001
Under ice shallow (°C)	Regression	0.61	0.03	19.13	<0.001
Density Δ (kg m ⁻³)	Regression	-0.05	0.01	-3.09	0.002
Intercept	Regression	0.01	0.01	0.59	0.557
Ice-off date					
Density Δ (kg m ⁻³)	Regression	-0.12	0.23	-0.50	0.614
Under ice shallow (°C)	Regression	0.00	1.68	0.00	0.999
Under ice deep (°C)	Regression	0.87	1.20	0.73	0.466
Heat content (MJ)	Regression	-0.81	2.67	-0.30	0.762
Intercept	Regression	0.01	0.19	0.06	0.955
Ice-off date					
Spring mixed period (d)	Covariance	-0.49	0.20	-2.43	0.015